UNIVERSITY OF PARDUBICE

FACULTY OF CHEMICAL TECHNOLOGY

Institute of chemistry and technology of macromolecular compounds

Martin Křižan

Development of new bispidone iron complexes useful as driers in oxidative drying paints

Theses of the Doctoral Dissertation

Pardubice 2019

Study program: **Chemistry and Technology of Materials**
Study field: **Surface Engineering**

Author: Martin Křižan
Supervisor: **prof. Ing. Jaromír Vinklárek, Dr.**
Year of the defence: 2019

References

KŘIŽAN, Martin. *Development of new bispidone iron complexes useful as driers in oxidative drying paints.* Pardubice, 2019. 112 pages. Dissertation thesis (Ph.D.). University of Pardubice, Faculty of Chemical Technology, Institute of Institute of Chemistry and Technology of Macromolecular Materials. Supervisors Prof. Ing. Jaromír Vinklárek, Dr.

Abstract

This dissertation is focused research and development of the new iron(II) bispidine complexes, which can be used as driers on the drying of air-drying paints. The theoretical part is described development of alkyd resins with regard to the environment, kinetic studies of drying alkyd resins, kind of driers and catalytic effect to autoxidation drying. The some part of theory is dedicated to 2D correlation of infrared spectra.

The experimental part is focused to synthesis and characterization of iron(II) complexes with modified bispidine ligand. The studied compounds were characterized by the help of FTIR and NMR spectroscopy. The series of intermediates, bispidine ligands
and iron(II) bispidine complexes were prepared. These compounds were characterized by the X-ray diffraction analysis. Simultaneously, catalytic effect of these compounds to drying of alkyd resins was studied. The FTIR was used as basic method for monitoring drying of alkyd resins.

From these studies, it is very clear that iron(II) complexes with modified bispidine ligand are appropriate substitutes for commercially available cobalt-based driers.

Abstrakt

Tato disertační práce je zaměřena na výzkum a vývoj nových bispidonových komplexů železa, která mohou být použita jako sikativy v oxidačně zasychajících nátěrových hmotách. V teoretické části je popsán vývoj alkydů s ohledem na ochranu životního prostředí, průběh zasychání alkydových pryskyřic, druhy sikativ a jejich katalyzované autooxidační procesy. Určitá část teoretické části je také věnována 2D korelacím infračervených spekter.

Experimentální část je zaměřena na syntézu a charakterizaci modifikovaných bispidinových komplexů železa. Studované sloučeniny byly charakterizovány pomocí infračervené spektroskopie (FTIR) a NMR spektroskopie. V rámci této disertační práce byla připravena série prekurzorů, bispidinových ligandů a bispidinových komplexů železa, která byla charakterizována pomocí rentgenové difrakční analýzy. Současně byl studován vliv připravených modifikovaných bispidinových komplexů na zasychání alkydových pryskyřicích. Základní technikou pro tuto studii byla FTIR, která byla doplněna 2D korelacemi infračervených spekter.

Ze získaných výsledků je zřejmé, že připravené modifikované bispidinové komplexy železa jsou potencionálními náhradami doposud komerčně používaných sikativ na bázi kobaltu.

Key words:

Autooxidation, driers, iron, bispidine, FTIR, NMR

Klíčová slova:

Autooxidace, sikativy, železo, bispidin, FTIR, NMR

Table of Contents

Introduction

This Thesis was focused on the studied of catalytic activity of drying of iron(II) complexes for the air-drying paints. Air-drying binders have been described as an important group of paints in modern organic coating. The main reaction centers in these molecules are double bonds. The reactions of these double bonds with air oxygen provide three-dimensional polymeric structure. This radical process, known as autoxidation, leads to conversion of the liquid paint layer to firm coating. Alkyd resins modified with highly unsaturated fatty acids are able to provide polymeric film without addition of any curing agents. This process is very slow and the resultant paint film has low hardness. However, the addition of the selected catalysts on based metal, called driers, enables to efficiently reduce the drying time. The shorter drying time lead to improvement the final properties of polymeric film [1, 2].

Industrially used driers are cobalt-based compounds, for example cobalt(II) 2-ethylhexanoate (**Co-Nuodex**). These driers are one of the most powerful drying agents, but proven toxicity of cobalt(II) compounds [3, 4] leads to replace these compounds with less toxic alternatives. The driers based on manganese [5, 6] or iron [7,8, 9] are known in the literature. These low toxic alternatives of driers have some undesirable properties, such as intensive color or lower activity at ambient temperature.[1] Recently, Fe-bispidon complex [10, 11] exhibited high drying effect and seems to be suitable not only for solvent-borne alkyd paints but also for water-borne binders. The finding of new, cheap and effective driers is still in progress.

Our research activity of the new drying agents leads us to organometallic iron compounds. High – valent iron complexes were explored as catalysts for oxidation and halogenation [12]. Selected iron complexes serves as an alternative for currently used cobalt (II) carboxylates those are under evaluation of European Chemical Agency owing to their toxic properties.[3, 4] Furthermore, the curing process, catalyzed by cobalt-free driers, is better controlled giving a more uniform distributionof the crosslinks [13]. The iron-based driers aren´t combined with secondary driers unlike vanadium-based driers. [2, 14]

1 Methods

The several experimental methods were used to determine drying activity and characterization of studied compounds. Due to the limited space of this annotation I will describe only selected of them which are the most important.

1.1 Film drying time

The drying performance of studied catalytic systems has been determined using a BYK Drying Time Recorder. The instrument is a straight-line recorder equipped with hemispherical ended needle (5 g weight used) that travels the length of the test strip under standard laboratory conditions (temperature 23°C, relative air humidity 50%). A glass test strip was prepared by casting a film upon it (thickness was 76 μm of wet film). The trace left on the film during the drying has been used to define tack free time (τ_1) and total dry time (τ_2). Three stages of the drying process were considered in accordance with literature [15]. During stage 1 (t = 0–τ_1), the paint flows together and starts to polymerize. It gives bold and uninterrupted line. During the stage 2 ($t = \tau_1$–τ_2), the surface is sticky and the path is ripped. After τ_2 (stage 3) the paint is through dry and needle travels on top of the surface and no trace in the film is observable. This method gives us information about drying activity of the studied driers at the beginning of the autoxidation.

1.2 Determination of film hardness

Film hardness development was monitored using a Persoz type pendulum (Elcometer Pendulum Hardness Tester, UK) in conformity with ISO 1522. The method is based on registering the number of pendulum swings it takes before the amplitude of the pendulum is damped to a certain extent. The more swings observed, the harder is the film. A plain glass test plate (10 × 20 cm) was coated with a 90 μm film (wet thickness) dried with the appropriate drier system and film hardness was measured within 100 days. The measured value was related to the hardness of a glass standard and expressed as relative hardness in percents. The error in determination of surface hardness was estimated to be ±0.5%. On summarizing of obtained data, dependence of film hardness versus time has been determined.

1.3 Time-resolved infrared spectroscopy

The autoxidation of alkyd resin was followed by time-resolved FTIR on spectrophotometers Nicolet 6700 and iS50 (32 scans per spectrum with a resolution of 2 cm^{-1}) in the range of 4000–500 cm^{-1}. Mixture of alkyd resin with appropriate drier was spread on the NaCl plate using an applicator with slot width 100 μm. Sample was placed in the spectrometer and IR spectrum was recorded each 5 min at 23 °C. Collected IR spectra were integrated using fixed two-point baseline in the region 3014–2997 cm^{-1} (cis-C=C-H stretch). Rate coefficients ($-k_{CH,max}$) at the beginning of the autoxidation process were estimated as the steepest slope of the logarithmic plot of the integrated area vs. time. The error in determination of $k_{CH,max}$ was less than 10% (three independent measurements for each run). The intensity of bands at 989 and 973

cm^{-1} was determined as the height of the band at these wavenumbers using linear baseline fixed at wavenumbers 1010 and 945 cm^{-1}.

1.4 2D correlation analysis

The generalized 2D correlation spectra were generated and processed by SpectraCorr 1.1 (Thermo Fisher Scientific). The analysis was performed on sets of spectra obtained from time-resolved FTIR experiments on 100 μm layer (wet width) at metal concentration 5×10^{-4} wt.% and 50 μm layer (wet width) at metal concentration 5×10^{-3} wt.%.

1.5 NMR spectroscopy

^{1}H and $^{13}C\{^{1}H\}$ NMR spectra were measured on a NMR spectrometer JNM-ECZ500R (Jeol) at room temperature. The chemical shifts are given in ppm relative to TMS. ^{13}C-DEPT135 and 2D techniques (^{1}H–^{1}H COSY, HSQC and HMBC) were used for assignment of signals in ^{1}H and $^{13}C\{1H\}$ NMR spektra.

2 Results and discussion

This part of Thesis is divided into two parts. The first part is focused on synthesis and characterization of studied compounds and second part is focused on influence prepared iron complexes to drying alkyd resins.

2.1 Synthesis and characterization of modified iron bispidine complexes

The quest for iron complex bearing pentadentate bispidine ligand with enhanced solubility in non-polar solvents led us to a new derivative decorated with long and branched alkyl tail. Such objective has achieved by a use of 2-ethylhexanoate that occupies the sixth position in the coordination sphere of iron. Although iron(II) 2-ethylhexanoate, necessary for synthesis of the title compound, has been reported previously [16], we decided to modify the synthetic procedure in attempt to avoid the potentially explosive inorganic perchlorate salts. Hence, our procedure uses in-situ neutralization of iron(II) hydroxide with 2-ethylhexanoic acid, see Scheme 1.

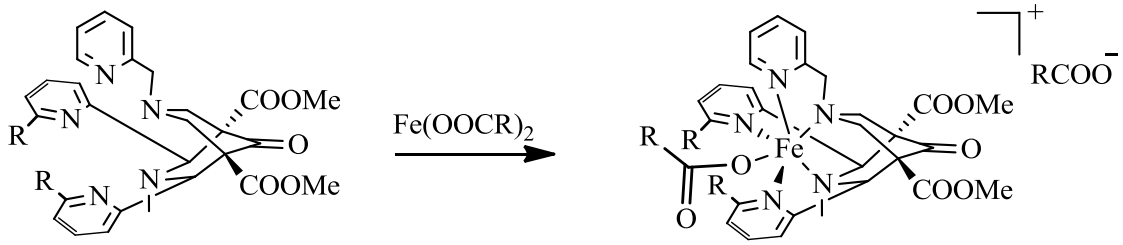

Scheme 1 Synthesis of bispidine iron complexes **FeL_1oct** and **FeL_2oct**

This product is unstabile on the air and therefore preparation and storage was carried out under an inert atmosphere. Identity and purity of the prepared product was characterized by the help of infrared spectroscopy. The characteristic band symmetric and antisymmetric valence vibrations of CH_3 and CH_2 groups (2960 cm^{-1}, 2959 cm^{-1}, 2877 cm^{-1}, 2875 cm^{-1}) were founded in the IR spektra. The characteristic band of the C-O vibration of carboxylic group (1529 cm^{-1}) was founded in IR spectra too.

The substituted and unsubstituted bispidin ligands were prepared by two one-pot Mannich condensation steps.[17, 18] In the first step, dimethyl-3-oxoglutarate reacts with methylamine and two equivalents of 6-R-pyridine-2-carboxaldehyde (R = H, Me, Br) to give apropriate substituted piperidone (**pL_1, pL_2, pL_3**, Scheme 2).

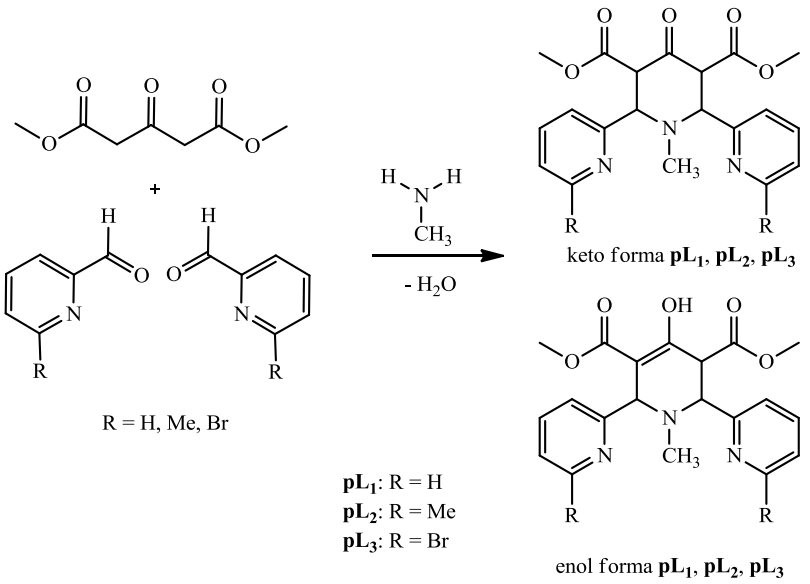

Scheme 2 Synthesis of bispidine intermediates pL_1, pL_2 and pL_3

In the second step precurzores pL_1, pL_2, pL_3 react with 2-(aminomethyl) pyridine and formaldehyde at elevated temperature. These condensations led to preparation appropriate bispidine ligand (L_1, L_2, L_3, Scheme 3).

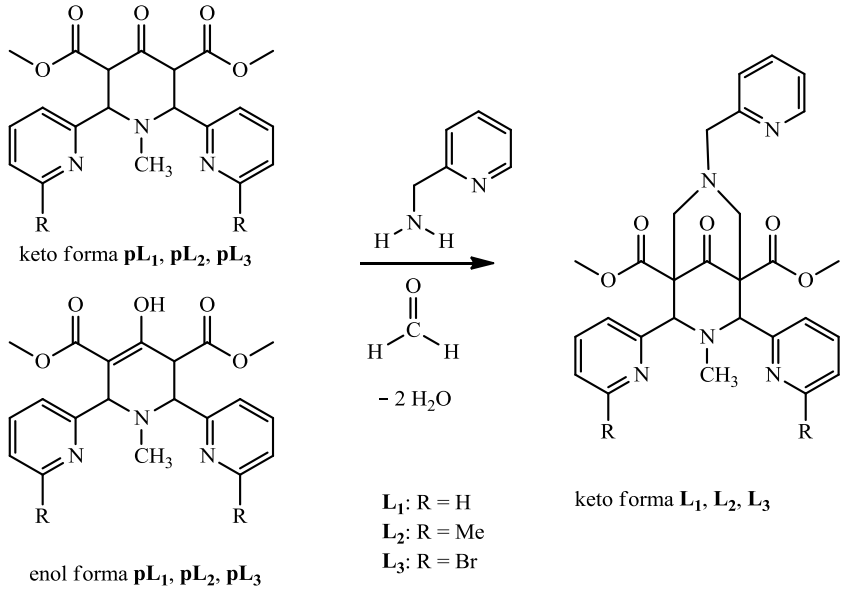

Scheme 3 Synthesis of bispidine ligands L_1, L_2, L_3

^{1}H NMR spectrum, measured in chloroform-d, proves appearance of enol and keto form in approximate molar ratio 4:1. ^{1}H NMR spectra of L_1, L_2, L_3 showed signals in range 9-7 ppm of the three pyridine rings and 5-1.9 ppm of the other parts of the molecule. In the vibration spectra of L_1, L_2, L_3 was found typical vibration for C=O of ester group (L_1 IR/Ra: 1735/1735 cm^{-1}, 1717/1724 cm^{-1} , L_2 IR/Ra: 1731/1734 cm^{-1}, 1721/1724 cm^{-1} , L_3 IR/Ra: 1733/1738 cm^{-1}, 1727/1724 cm^{-1}) and vibration for C=C of pyridine structure (L_1 IR/Ra: 1589/1593 cm^{-1}, 1571/1575 cm^{-1} , L_2 IR/Ra: 1592/1593 cm^{-1}, 1572/1575 cm^{-1} , L_3 IR/Ra: 1578/1577 cm^{-1}, 1554/1556 cm^{-1}).

Synthesis of the modified bispidine iron complexes **FeL_xoct** (x = 1, R = H; x = 2, R = Me) is based on reaction bispidine ligand L_1 or L_2 with iron(II)

2-ethylhexanoate under the inert atmosphere (see Scheme 1). Product of this reaction (**FeL_xoct**) is formed by cationic species $[Fe(bispi)(2\text{-ethylhexanoate})]^+$ compensated anionic species $[(2\text{-hexanoate})]^-$. In the case preparation of bispidine complex substituted by bromine, failed to prepar relevant iron complex. The reason for the complexity of this complex is, that there is no-coordination under given conditions.

The modified bispidine iron complexes **FeL_xoct** were chraracterization by the help of IR spectroscopy, Mass spectroscopy and X-ray difraction analysis. I mention in this part only about few characterized information of them. **FeL_1oct** was recrystallized from mixture CH_2Cl_2 and Et_2O and this process has provide **FeL_1oct·0.75CH_2Cl_2**. The structure of **FeL_1oct·0.75CH_2Cl_2** was confirmed by the X-ray diffraction analysis. Infrared absorption bands, characteristic for the presence of ester and carboxylate groups, have been found in the region 1730–1600 cm^{-1}. Broadened bands at 2654 and 2554 cm^{-1} are due to hydroxyl functions involved in strong hydrogen bond. At the same time the monocrystalic materials was obtained careful overlap acetonitrile solution **FeL_2oct** by Et_2O. This molecular structure was confirmed by X-ray diffraction analysis too. Infrared absorption bands, characteristic for the presence of ester and carboxylate groups, have been found in the region 1730–1600 cm^{-1}. Broadened bands at 2654 and 2554 cm^{-1} are due to hydroxyl functions involved in strong hydrogen bond. The very rigid nature of the bispidine complexes **FeL_1oct·0.75CH_2Cl_2** and **FeL_2oct** is well demonstrated on the structural parameters Fe–N and N–Fe–N, which are virtually identical to those previously reported for complexes $[Fe(bispi)Cl]Cl\cdot H_2O$ and $[Fe(bispi)SO_4]\cdot 2MeOH$ [12] (Table 1 and Table 2).

Table 1 Selected binding lenght [Å] describing coordination sphere of iron in **FeL_1oct, FeL_2oct**, **FeL_1Cl**, **FeL_1SO_4**

	Binding lenght [Å]			
	FeL_1oct	**FeL_2oct**	**FeL_1Cl**[12]	**FeL_1SO_4**[12]
Fe1-N1	2.195 (4)	2.195 (5)	2.194 (2)	2.181 (2)
Fe1-N2	2.338 (4)	2.313 (3)	2.362 (2)	2.376 (2)
Fe1-N3	2.172 (5)	2.221 (3)	2.142 (2)	2.192 (2)
Fe1-N4	2.228 (3)	2.347 (4)	2.182 (2)	2.143 (2)
Fe1-N5	2.158 (3)	2.185 (4)	2.134 (2)	2.129 (2)
Fe1-O1	1.981 (4)	1.993 (5)		2.015 (2)
Fe1-Cl1			2.416 (1)	

Table 2 Selected binding angle [°] describing coordination sphere of iron in **FeL_1oct, FeL_2oct**, **FeL_1Cl**, **FeL_1SO_4**

	Bainding angle [°]			
	FeL_1oct	**FeL_2oct**	**FeL_1Cl**[12]	**FeL_1SO_4**[12]
O1-Fe1-N2	173.15 (2)	167.52 (1)		
N1-Fe1-N2	79.15 (1)	77.32 (1)	78.27 (5)	78.27 (7)
N1-Fe1-N5	153.36 (2)	155.24 (1)		
N2-Fe1-N3	88.02 (1)	87.18 (9)	86.15 (5)	88.82 (8)
N2-Fe1-N4	89.84 (1)	91.57 (9)	94.12 (5)	86.08 (7)
N2-Fe1-N5	77.33 (1)	77.33 (1)	76.00 (5)	78.39 (8)
N3-Fe1-N4	151.39 (2)	151.56 (1)	151.82 (6)	155.55 (9)
N3-Fe1-N5	76.70 (1)	76.15 (1)	76.48 (6)	77.15 (8)

2.2 The effect of the $FeL_1oct \cdot 0.75CH_2Cl_2$ and FeL_2oct to drying alkyd resins

Excellent solubility of **FeL_xoct** in solvent borne alkyd resins enables to study its drying activity in a wide range of concentrations without necessity of pre-dissolving. The performance of the complex was studied in solvent-borne phthalic-type alkyd resins of different oil length modified with soybean oil (**S40**, **S50** and **S60**). We observed drying times (τ_1 and τ_2) and relative hardness of the alkyd films ($H_{rel,5d}$ and $H_{rel,100d}$) for formulations with a different concentration of the drier. At the same time we observed drying mechanism by the help of IR spectroscopy.

2.2.1 Mechanical properties

2.2.1.1 Alkyd resin of short oil lenght

Catalytic aktivity of substituted and unsubstituted **FeL_xoct** complexes were compared with commercial available **Co-Nuodex**. In case of **Co-Nuodex** manufacturer recommend dosing 0.1 wt% for all of used alky resins (**S40**, **S50** and **S60**). O. Preininger described faster drying of alkyd resin of short oil length (**S40**) while dosing 0.06 wt% commercial drier **Co-Nuodex** unlike recommended amount by manufacturer. For this reason, the results will be compared with this concentration.[19]

The measurement results of drying alkyd resin of short oil length (**S40**) using different concentration **FeL_1oct**, it is evident that this complex has very goog drying activity at the wide range concentrations. The shortes drying times were achieved using concentration 5×10^{-2} wt% **FeL_1oct** for first step and total drying time. These times are significantly shorter than times founded for optimal concentration **Co-Nuodex** (τ_1 0.8 h and τ_2 3.1 h **FeL_1oct**, τ_1 2.7 h and τ_2 6.9 h **Co-Nuodex**). The higher drying speed was reflected of relative hardness of film, which initially shows higher quantity (37.2 %) against commercial cobalt-based drier (23.3 %). The values of relative hardness after 100 days reache 49.8% in case **FeL_1oct** and 58.5 % for **Co-Nuodex**. Finally, the results our research show that ideal concentration of **FeL_1oct** is 1×10^{-3} wt%, so us to achieve the same activity as cobalt-based drier. This concentration led to getting total drying time 6.5 h and relative hardness after 100 days 51.1 % (for **Co-Nuodex** 6.9 h and 58.5 %). Due to this fact is it possible reduces the

absolut amount of drying agent used and while maintaining almost the same mechanical properties.

In the case of substituted **FeL_2oct** was observed effect of methyl groups to drying aktivity. This complex has catalytic effects in a smaller concentration range (from 5 x 10^{-2} to 5 x 10^{-3} wt.%, when the total drying time was to 10 h. The concentration 5 x 10^{-2} wt·% exhibits similar drying properties as commercial using **Co-Nuodexu** (0.1 wt.%). The drying time at the first step is slightly faster (3h), but total drying time (7.6 h) is almost identical as commercial cobalt-based drier (τ_1 = 5.5 h, τ_2 = 7.6 h). The relative hardness of film with using **FeL_2oct** is a few percent higher in the first phase (23.1 %) and significantly lowers after 100 days (51.1 %) than **Co-Nuodex** (5 days 20.1 % a 100 days 61.2 %).

Table 3 Drying times and relative hardness of film of alkyd resin **S40** ([a] Drying time. [b] Total drying time. [c] Relative hardness after 5 days. [d] Final relative hardness after 100 days).

FeL_1oct				
Fe conc.	τ_1 [a]	τ_2 [b]	$H_{rel.}$ [c] 5d	$H_{rel.}$ [d] 100d
wt.%	(h)	(h)	(%)	(%)
5 x 10^{-2}	0.8	3.1	37.2	49.8
1 x 10^{-2}	3.1	4.2	37.0	48.9
5 x 10^{-3}	0.8	3.3	34.2	47.5
1 x 10^{-3}	4.6	6.5	39.4	51.1
5 x 10^{-4}	6.2	6.9	35.2	47.4

FeL_2oct				
Fe conc.	τ_1 [a]	τ_2 [b]	$H_{rel.}$ [c] 5d	$H_{rel.}$ [d] 100d
wt.%	(h)	(h)	(%)	(%)
5 x 10^{-2}	3.0	7.6	23.1	51.1
1 x 10^{-2}	4.2	8.1	24.3	49.9
5 x 10^{-3}	6.9	8.6	24.7	50.4
1 x 10^{-3}	20.8	>24	24.4	50.4
5 x 10^{-4}	>24	>24	24.4	51.1

Commercial driers					
	conc. metal	τ_1 [a]	τ_2 [b]	$H_{rel.}$ [c] 5d	$H_{rel.}$ [d] 100d
	wt.%	(h)	(h)	(%)	(%)
Co Nuodex[19]	1 x 10^{-1}	5.5	7.6	20.1	61.2
Co Nuodex[19]	6 x 10^{-2}	2.7	6.9	23.3	58.5
BORCHI®OXY – Coat (Fe)	5 x 10^{-3}	0.4	9.9	-	-
BORCHI®OXY – Coat (Fe)	1 x 10^{-3}	0.8	6.7	-	-

2.2.1.2 Alkyd resin of medium oil length

Symultaneously, we studied catalytic effect of **FeL_1oct** and **FeL_2oct** ondrying time alkyd resin of medium oil lenght. The measurements on the alkyd resin of medium oil length (**S50**) revealed excellent catalytic activity of the **FeL_1oct** at considerably lower range of metal concentrations 1×10^{-2} to 5×10^{-4} wt.% (Table 4) than recommended for the commercial cobalt-based drier Co-Nuodex (1×10^{-1} wt.%). Hence, within this range, the alkyd coatings are dry in less than 7 h and their final relative hardness, measured 100 days after the application, varies between 44.4% and 48.9% of the glass standard. Furthermore, the fresh coatings become firm after few days of the drying as evident from the $H_{rel,5d}$ values, see Table 4. The optimal drying performance of the **FeL_1oct** was achieved in the run **C**, as evidenced by short tack-free time (τ_1 =0.8 h) and total dry time (τ_2 = 4.6 h). The use of lower concentrations led to gradual prolongation of the drying process. Nevertheless, the performance of the **FeL_1oct** at the lower metal concentration (run **E**) is still comparable to formulations at the optimal dosage of **Co-Nuodex**.[19] The deterioration of the catalytic activity was observed only below concentration 5×10^{-4} wt.% (run F) and is apparent from the long total dry times exceeding 24 h. Using iron concentrations higher than 5×10^{-3} wt.% (runs **A** and **B**), caused overdosing as evident from longer total dry times (τ_2). At these concentrations, the autoxidation process is probably decelerated due to thin polymeric layer on the top surface of the alkyd film hindering the oxygen diffusion into the coating. Very similar behavior was observed at concentration 1 x 10^{-1} wt.% **FeL_2oct** (τ_1 = 0.7 h and τ_2 = 10 h). Finally, in the case **FeL_1oct** optimal concentration was 5 x 10^{-3} wt.% (τ_1 = 0.8 h and τ_2 = 4.6 h) and for **FeL_2oct** was 1 x 10^{-2} wt.% (τ_1 = 0.8 h and τ_2 = 4.9 h), see Table 4. Both of these iron-based driers proved higher catalytic activity than **Co-Nuodex** (τ_1 = 5.2 h and τ_2 = 6.7 h). The relative hardness all of dried films have similar value after 100 days (**FeL_1oct** 46.7 ± 2.3 %, **FeL_2oct** 50.7 ± 2.1 %), although in the early days of drying, relatively increasing hardness values were observed at lower concentrations.

Table 4 Drying times and relative hardness of film of alkyd resin **S50** ([a] Drying time. [b] Total drying time. [c] Relative hardness after 5 days. [d] Final relative hardness after 100 days).

FeL_1oct				
Fe conc.	τ_1 [a]	τ_2 [b]	$H_{rel.\ 5d}$ [c]	$H_{rel.\ 100d}$ [d]
wt.%	(h)	(h)	(%)	(%)
5×10^{-2}	0.8	11.5	19.2	46.8
1×10^{-2}	0.9	5.0	20.1	48.9
5×10^{-3}	0.8	4.6	19.0	46.7
1×10^{-3}	1.5	6.2	26.4	46.7
5×10^{-4}	1.5	6.5	27.1	44.4
1×10^{-4}	22.3	>24	-	-

FeL_2oct				
Fe conc.	τ_1 [a]	τ_2 [b]	$H_{rel.\ 5d}$ [c]	$H_{rel.\ 100d}$ [d]
wt.%	(h)	(h)	(%)	(%)
1×10^{-1}	0.7	10.0	18.2	52.8
5×10^{-2}	0.9	6.2	20.3	52.0
1×10^{-2}	0.8	4.9	21.0	51.5
5×10^{-3}	1.7	5.4	26.3	49.9
1×10^{-3}	2.3	6.9	27.6	48.7

Comercial driers					
	conc. metal	τ_1 [a]	τ_2 [b]	$H_{rel.\ 5d}$ [c]	$H_{rel.\ 100d}$ [d]
	wt.%	(h)	(h)	(%)	(%)
Co Nuodex[19]	1×10^{-1}	5.2	6.7	14.7	54.1
BORCHI®OXY – Coat (Fe)	5×10^{-3}	1.0	3.23	-	-
BORCHI®OXY – Coat (Fe)	1×10^{-3}	2.6	7.1	-	-

2.2.1.3 Alkyd resin of long oil length

Finally, we studied catalytic activity of **FeL_1oct** and **FeL_2oct** on drying alkyd resin of long oil lenght (**S60**). This studies has proven that even hoigh concentration Fe (0.1 wt. %) do not lead to overdosing. The optimal concentration of both iron-based driers is 1×10^{-1} wt.%, when total drying times are shorter 4 hours (**FeL_1oct** τ_2 = 3.9 h, **FeL_2oct** τ_2 = 3.1 h), see Table 5). For comparison, total drying for comercial using **Co-Nuodex** is at concentration 4.6 h. The result suggest that **FeL_2oct** has higer drying aktivity at concentration range 1×10^{-1} to 1×10^{-2} wt.%, see Table 5). The development of relative hardness at time has both of iron-based driers very similar values (**FeL_1oct** 27.9 ± 2.2 %, **FeL_2oct** 26.6 ± 3.1 %). For commercially avaliable **Co-Nuodex (**0.1 wt.%) is known relative hardness of film 39.4 %.

Table 5 Drying times and relative hardness of film of alkyd resin **S60** ([a] Drying time. [b] Total drying time. [c] Relative hardness after 5 days. [d] Final relative hardness after 100 days)

FeL_1oct				
Fe conc.	τ_1 [a]	τ_2 [b]	$H_{rel.}$ [c] 5d	$H_{rel.}$ [d] 100d
wt%	(h)	(h)	(%)	(%)
1×10^{-1}	0.8	3.9	16.7	30.1
5×10^{-2}	1.5	6.1	16.0	30.0
1×10^{-2}	5.4	8.5	15.1	28.2
5×10^{-3}	9.2	10.4	15.4	27.8
1×10^{-3}	>24	>24	11.0	25.7

FeL_2oct				
Fe conc.	τ_1 [a]	τ_2 [b]	$H_{rel.}$ [c] 5d	$H_{rel.}$ [d] 100d
wt.%	(h)	(h)	(%)	(%)
1×10^{-1}	1.8	3.1	17.4	30.2
5×10^{-2}	2.7	5.0	16.3	30.0
1×10^{-2}	5.4	7.1	14.3	27.9
5×10^{-3}	6.9	10.8	14.2	26.9
1×10^{-3}	23.1	>24	14.1	23.8

Comercial driers					
	conc. metal	τ_1 [a]	τ_2 [b]	$H_{rel.}$ [c] 5d	$H_{rel.}$ [d] 100d
	wt.%	(h)	(h)	(%)	(%)
Co Nuodex[19]	1×10^{-1}	0.8	4.6	9.3	39.4
BORCHI®OXY – Coat (Fe)	1×10^{-2}	0.8	4.6	-	-
BORCHI®OXY – Coat (Fe)	5×10^{-3}	0.8	4.8	-	-

2.2.2 FTIR spectroscopy

Time-resolved FTIR spectroscopy was used for the monitoring of the autoxidation process. The main attention was given to the symmetrical CH stretching band of the *cis*-CH=CH moiety at 3008 cm^{-1}, whose disappearance is routinely used as a tool for determination of the rate of the autoxidation process.[5, 9, 20] Hence, its integrated area well correlates with concentration of the reactive moiety bearing isolated double bonds that rearranges during the autoxidation to conjugated double bond system (see ROOH in Scheme 3).[1] The band at 989 cm^{-1}, assigned to C-H wagging of the cistrans conjugated double bond system,[21] rises steeply at the beginning of the autoxidation process as the hydroperoxides are formed. Their decomposition followed with simple recombination reactions yielding ROOR, ROR and RR crosslinks[2] do not influence the band intensity since the conjugated double bond system stays untouched. Nevertheless, concentration growth of the conjugated double bonds enhances the chance for radical addition reactions. Subsequently, the

appeared conjugated double bonds are consumed producing moiety with isolated trans-double bond, which concentration is proportional to the intensity of the band at 973 cm^{-1} (C=C-H wagging).[21]

2.2.2.1 Alkyd resin of short oil length

At the beggining we wtched changes of vibration band at 3008 cm^{-1} of alkyd resin **S40**. As an example of the alkyd resin **S40**, the time evolution of the integral vibration intensity of the band at 3008 cm^{-1} can be seen depending on the different concentration of **FeL_1oct** (see Figure 2 on the left). A significant decrease in band intensity was observed with $1x10^{-2}$ wt. % (**B**), $5x10^{-3}$ wt. % (**C**), $1x10^{-3}$ wt. % (**D**), $5x10^{-4}$ wt. % (**E**), resulting in half of the substrate being consumed within the first few hours, which correlates well with the short drying time (see Table 6). In case of concentration $5x10^{-2}$ wt. % (**A**) is shown to be overdosing using excessive amounts of **FeL_1oct** drier. This slows down the reaction rate before reaching 50 % (see Figure 2, left, curve A). The graph of integral dependence of concentration B shows to a slight overdosing that only slightly deflects the ideal curve.

Previous kinetic experiments on the ethyl linoleate model system suggest that the onset of the autooxidation process can be considered a pseudo-first order reaction.[22] However, it can only be used as an approach for liquid oxygenated systems. In the case of alkyd binders, these conditions are fulfilled to approximately 50% conversion ($t \leq t_{50\%}$), which corresponds to the moment when the system solidifies and oxygen diffusion becomes the determining process.

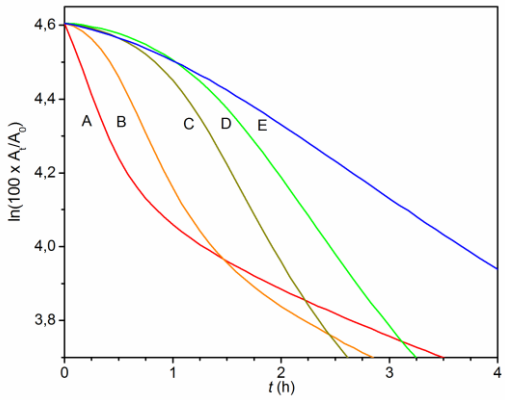

Figure 1 Time dependence of the integral area of band at 3008 cm^{-1} on logarithmic scale in the S40 system and various concentrations of **FeL_1oct.**

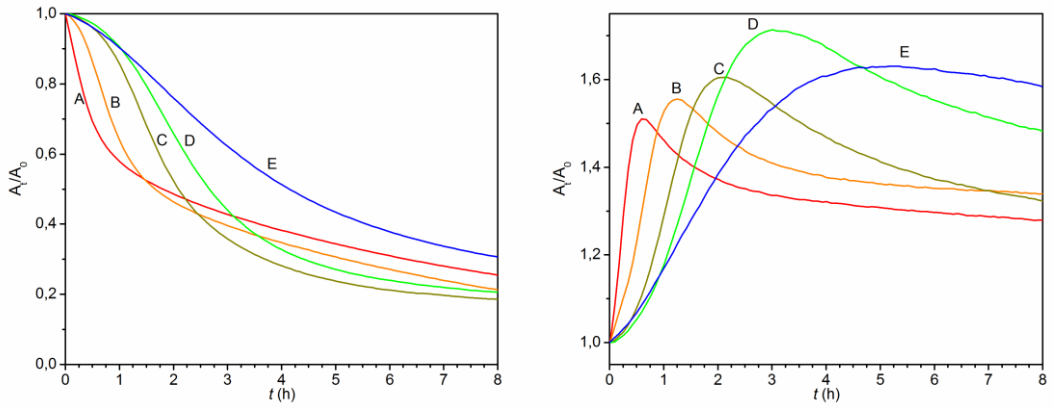

Figure 2 Time dependence of the relative integral area of the band at 3008 cm $^{-1}$ (left) and the graph of the time dependence of the relative absorbance of the band at 989 cm $^{-1}$ (right) in the S40 system and various concentrations of **FeL$_1$oct.** The metal concentration used is shown in Table 6.

For **B-E** systems, the logarithmic time dependence is almost linear with a very short induction time (IT = 0.11 - 0.56 h) (see Figure 1). In accordance with the obtained drying times (τ), it is evident that increasing the concentration leads to an increase in the reaction coefficients and a shortening of the induction time. At a higher concentration of metals (System **A**), there is evidence of overdosing of the drier and deviate from linearity. This deviation is already apparent at 40% conversion (see Figure 2 on the left). Although this system provides the highest rate constant ($-k_{CH,\ max}$ = 0.80 h^{-1}), the autooxidation of the alkyd becomes less effective after about 1.5 hours, because oxygen consumption is higher than its diffusion into the layer even at low substrate conversion. Surface autooxidation is likely to be too rapid, resulting in the rapid formation of a strongly crosslinked surface film that greatly slows oxygen diffusion.

As mentioned above, during autooxidation, isolated double bonds are converted to conjugated double bonds. Figure 2 (right) shows, how the conjugated double bond concentration increases at the beginning of the autooxidation process. At the moment of enough of these reactive sites, the radicals start attacking them. As the time of these attacks increases, the number of addition reactions is equal to the reactions producing the conjugated bonds and the bandwidth of 989 cm^{-1} reaches its maximum ($t_{conj.}$). Addition reactions are already predominant from this point, and the CH band of the conjugated double bond system begins to lose intensity.

The shortest time required to reaching the maximum band at 989 cm^{-1} was achieved for concentration **A** at 0.59 h, while the highest band intensity reached **D** concentration about 2.5 hours later. This suggests that, in the short alkyd**, FeL$_1$oct** not only promotes the degradation of peroxidic bonds but also crosslinking reactions. All of obtained data are listed in the Table 6.

Table 6 Kinetical data autooxidation process of alkyd resin **S40** with different concentration drier **FeL$_1$oct** ([b] Total-dry time. [e] Maximum oxidation rate constant ($k_{CH,max}$). [f] Time has been determined as point when 5, 50 and 90% of active CH bonds is consumed. [g] Drying time in which the band at 989 cm^{-1} reached maximal absorbance. IP Induction period.)

	FeL$_1$oct								
	Fe conc. wt.%	$-k_{CH.\,max}$ [e] (h^{-1})	t_{max} [e] (h)	$t_{5\%}$ [f] (h)	$t_{90\%}$ [f] (h)	$t_{conj.}$ [g] (h)	$t_{50\%}$ [f] (h)	IP (h)	τ_2 [b] (h)
A	5 x 10^{-2}	0.80	0.17	0.05	25.7	0.59	1.9	0.05	3.1
B	1 x 10^{-2}	0.63	0.75	0.25	11.6	1.26	1.65	0.11	4.2
C	5 x 10^{-3}	0.54	1.67	0.61	22	2.17	2.1	0.43	3.3
D	1 x 10^{-3}	0.42	2.1	0.67	69.7	3.01	2.66	0.53	6.5
E	5 x 10^{-4}	0.21	2.59	0.68	71	5.26	4.1	0.56	6.9

Addition of radicals to conjugated double bonds results in crosslinking of fatty acids and formation of a film. In this process, isolated double bonds are formed and their increasing amount corresponds to increasing bandwidth at 974 cm^{-1}. Figure 3 (left) display the development of isolated double bonds with time using different concentrations of **FeL$_1$oct**.

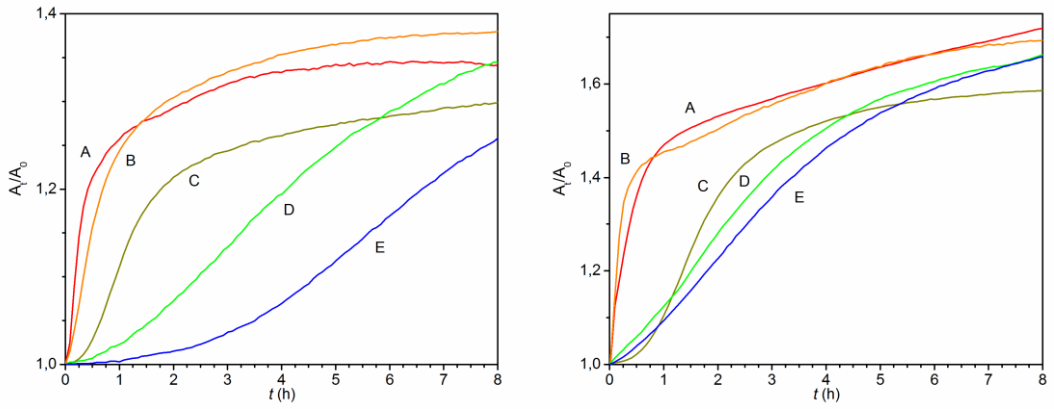

Figure 3 Time dependence of relative integral strip area at 974 cm $^{-1}$ (left) and graph showing development of OH vibrations of hydroxy and peroxy groups over time (right) in the **S40** system and various concentrations of **FeL$_1$oct**. The metal concentration is shown in Table 6.

The last part of the IR spectrum was studied area 3650-3125 cm^{-1}. Whereas the each alkyd resin contains unreacted carboxylic acid residues or OH alcohol groups, a broad band is found in the region of interest. The maximum of the band is approximately 3520 cm^{-1}. Hydroperoxide and alcohol groups are formed during the autoxidation process. The vibrations of their OH groups appear in the spectrum at 3410 cm^{-1} (hydroperoxide), 3520 and 3300 cm^{-1} (free and bound OH groups). These vibrations are added to the original belt, which over time increases with a new

maximum at 3436 cm^{-1}. Figure 3 (right) shows the increase in the integral area of this wide band with time for different concentrations of the **FeL_1oct**.

In the case **FeL_2oct**, as potential drier, changes in the IR spectrum were studied. The monitoring of system **FeL_2oct/S40** at different concentrations ($5x10^{-2}$ wt.% (**A**), $1x10^{-2}$ wt. % (**B**), $5x10^{-3}$ wt.% (**C**), $1x10^{-3}$ wt.% (**D**), $5x10^{-4}$ wt.% (**E**)) gave almost ideal results of drying kinetics. These results for **FeL_2oct/S40** are different against **FeL_1oct/S40**, when the conversion of isolated double bonds to conjugated double bonds is addicted of concentration. The obtained data are shown in the Table 7.

Table 7 Kinetical data autooxidation process of alkyd resin **S40** with different concentration drier **FeL_2oct** ([b] Total-dry time. [e] Maximum oxidation rate constant ($k_{CH,max}$). [f] Time has been determined as point when 5, 50 and 90% of active CH bonds is consumed. [g] Drying time in which the band at 989 cm^{-1} reached maximal absorbance. IP Induction period.)

	FeL_2oct								
	Fe conc.	$-k_{CH.\ max}$ [e]	t_{max} [e]	$t_{5\%}$ [f]	$t_{90\%}$ [f]	$t_{conj.}$ [g]	$t_{50\%}$ [f]	IP	τ_2 [b]
	wt.%	(h^{-1})	(h)	(h)	(h)	(h)	(h)	(h)	(h)
A	5×10^{-2}	1.21	1.10	0.50	9.30	1.43	1.37	0.17	7.6
B	1×10^{-2}	0.21	7.52	2.78	41	8.69	7.77	1.12	8.1
C	5×10^{-3}	0.13	13.64	6.40	70	16.142	14.88	4.65	8.6
D	1×10^{-3}	0.09	21.89	9.26	>70	24.29	21.00	8.24	>24
E	5×10^{-4}	0.08	29.80	14.80	>70	33.382	31.24	11.83	>24

2.2.2.2 Alkyd resin of medium oil lenght

The obtained data for concentrations $5x10^{-3}$ wt.% (**C**), $1x10^{-3}$ wt.% (**D**), $5x10^{-4}$ wt.% (**E**) of **FeL_1oct** showed that a logarithmic time dependence almost linear with a very short induction time (IT = 0.2 - 0.6 h) (see Figure 7 on the right). From measured values of drying time (τ) was found that increasing concentration leads to an increase reaction coefficients and shortening of induction time. The higher concentration of metal ($1x10^{-2}$ wt.%, system **B**) proves the first signs of overdose. This system provides the highest rate constant ($-k_{CH,max}$ = 1.24 h^{-1}) and autoxidace is less effective. The higher concentration of iron-based drier ($5x10^{-2}$ wt.%, system **A**) decreases reaction coefficients ($-k_{CH,max}$ = 0.7 h^{-1}) and slows down katalytic process. In the case of alkyd resin **S50** in which high concentration of drier leads to shortening $t_{conj.}$ (see Table 8). Interestingly, the value is not influence by overdosing and it is contrary with kinetics parameters associated with the formation of hydroperoxides (např. $-k_{CH,max}$, t_{max}, $t_{1/2}$).

Table 8 Kinetical data autooxidation process of alkyd resin **S50** with different concentration drier **FeL_1oct** ([b] Total-dry time. [e] Maximum oxidation rate constant ($k_{CH,max}$). [f] Time has been determined as point when 5, 50 and 90% of active CH bonds is consumed. [g] Drying time in which the band at 989 cm^{-1} reached maximal absorbance. IP Induction period.)

	FeL_1oct								
	Fe conc. wt.%	$-k_{CH.\,max}$ [e] (h^{-1})	t_{max} [e] (h)	$t_{5\%}$ [f] (h)	$t_{90\%}$ [f] (h)	$t_{conj.}$ [g] (h)	$t_{50\%}$ [f] (h)	IP (h)	τ_2 [b] (h)
A	5×10^{-2}	0.7	0.18	0.18	>40	0.34	13.1	0.093	11.5
B	1×10^{-2}	1.24	0.25	0.09	12.4	0.51	0.98	0.095	5.0
C	5×10^{-3}	0.78	0.76	0.26	18.2	1.18	1.21	0.17	4.6
D	1×10^{-3}	0.51	1.68	0.43	37	1.84	1.89	0.29	6.2
E	5×10^{-4}	0.32	2.76	0.76	40	3.85	3.17	0.63	6.5
F	1×10^{-4}	0.02	64	33	>90	>90			>24

The experiments made by **FeL_2oct** and using alkyd resin **S50** proved, that is necessary the higer concentration than **FeL_1oct**. All of the using concentrations of iron-based drier ($1x10^{-1}$ (**A**), $5x10^{-2}$ (**B**), $1x10^{-2}$ (**C**), $5x10^{-3}$ (**D**), $1x10^{-3}$ (**E**) wt. %.) reported katalytic activity, but the optimal cocncetration is showen 1×10^{-2} wt. % (**C**). All of collected data are summarize in Table 9.

Table 9 Kinetical data autooxidation process of alkyd resin **S50** with different concentration drier **FeL_2oct** ([b] Total-dry time. [e] Maximum oxidation rate constant ($k_{CH,max}$). [f] Time has been determined as point when 5, 50 and 90% of active CH bonds is consumed. [g] Drying time in which the band at 989 cm^{-1} reached maximal absorbance. IP Induction period.)

	FeL_2oct								
	Fe conc. wt.%	$-k_{CH.max}$ [e] (h^{-1})	t_{max} [e] (h)	$t_{5\%}$ [f] (h)	$t_{90\%}$ [f] (h)	$t_{conj.}$ [g] (h)	$t_{50\%}$ [f] (h)	IP (h)	τ_2 [b] (h)
A	1×10^{-1}	0.18	1.81	0.97	>90(130)	3.01	19	0.2	10.0
B	5×10^{-2}	0.50	0.68	0.31	36.52	1.55	3.35	0.7	6.2
C	1×10^{-2}	0.58	2.18	0.82	14.2	1.82	2.30	1.2	4.9
D	5×10^{-3}	0.14	9.19	3.6	59	11.6	10.1	3.5	5.4
E	1×10^{-3}	0.10	13.36	5.55	88	15.53	15.00	5.0	6.9

2.2.2.3 Alkyd resin of long oil lenght

The last part of our study was focused on using **FeL$_x$oct** as drier for alkyd resin of long oil length (**S60**). The kinetic data of system **FeL$_x$oct /S60** proved that relative low effectivity of iron-based driers isn´t caused by low solubility in thealkyd resin, but their low catalytic acitivity in the media of alkyd. The value of -$k_{CH,max}$ increases with increasing concentration of metal for all of experiments, when it is possible to rule out loss of activity due to overdosing or depending on the presence of undissolved drier. Although the alkyd studied resins are structurally similar and contain identical active substrates, the higher content of fatty acid in the **S60** alkyd resin dramatically reduces its polarity. In our case, this is likely to complicate the transition between the two oxidation states in the redox system FeII / FeIII and slow down the cleavage of ROOH, a process necessary for autooxidation of the binder.

In the case of alkyd resin of long oil length **S60** is necessary using higer concentration of driers than **S40** and **S50**, to be achieved similar result of drying. The concentrations 1 x 10^{-1} (**A**), 5 x 10^{-2} (**B**), 1 x 10^{-2} wt.% (**C**) of **FeL$_1$oct** reported suitable drying time (8h) (see Table 10). The concentrations **A** and **B** report relatively low inhibitory period (0.8-1.1h) and reached their maximum conjugated double bonds at the same time (2.52/2.76 h). Compared to that concentrations **C** and **D** (5 x 10^{-3} wt. %) was observed a decrease drying activity as a result low quantity drier in the system. The low quantity of **FeL$_1$oct** in the system leads to extension total drying time (8.5 h (**C**), 10.4 h (**D**)) and the maximum of intensity of band of conjugated double bond reaches large value (13.8 h (**C**), 22.9 h (**D**)) (see Table 10).

Table 10 Kinetical data autooxidation process of alkyd resin **S60** with different concentration drier **FeL$_1$oct** ([b] Total-dry time. [e] Maximum oxidation rate constant ($k_{CH,max}$). [f] Time has been determined as point when 5, 50 and 90% of active CH bonds is consumed. [g] Drying time in which the band at 989 cm^{-1} reached maximal absorbance. IP Induction period.)

	FeL$_1$oct								
	Fe conc. wt.%	-$k_{CH.\ max}$ [e] (h^{-1})	t_{max} [e] (h)	$t_{5\%}$ [f] (h)	$t_{90\%}$ [f] (h)	$t_{konj.}$ [g] (h)	$t_{50\%}$ [f] (h)	IP (h)	τ_2 [b] (h)
A	1 x 10^{-1}	0.49	2.01	1	40.7	2.52	2.37	0.81	3.9
B	5 x 10^{-2}	0.33	2.09	1.7	65	2.76	3.47	1.1	6.1
C	1 x 10^{-2}	0.11	8.44	4.68	65	13.77	11.8	4.5	8.5
D	5 x 10^{-3}	0.06	14.00	7.6	>70	22.89	20.79	6.5	10.4

The experimetr executed with **FeL$_2$oct** as drier was achieved very similar results like **FeL$_1$oct**. The good drying activity was achieved with concentrations 1 x 10^{-1} (**A**), 5 x 10^{-2} (**B**), 1 x 10^{-2} wt.% (**C**) (Table 11). The continuous reduction of concentration drier (5 x 10^{-3} **D**, 1 x 10^{-3} wt.% **E**) led to extension total drying time over 8 h (see Table 11). Nevertheless, the speed constant of concentrations **A**, **B** and **C**

of **FeL$_2$oct** are higher than the speed constants while using **FeL$_1$oct** and total drying time are almost identical. The other obtained data are reported at Table 11.

Table 11 Kinetical data autooxidation process of alkyd resin **S60** with different concentration drier FeL$_2$oct ([b] Total-dry time. [e] Maximum oxidation rate constant ($k_{CH,max}$). [f] Time has been determined as point when 5, 50 and 90% of active CH bonds is consumed. [g] Drying time in which the band at 989 cm^{-1} reached maximal absorbance. IP Induction period.)

	FeL$_2$oct								
	Fe conc.	$-k_{CH.\ max}$ [e]	t_{max} [e]	$t_{5\%}$ [f]	$t_{90\%}$ [f]	$t_{conj.}$ [g]	$t_{50\%}$ [f]	IP	τ_2 [b]
	wt.%	(h^{-1})	(h)	(h)	(h)	(h)	(h)	(h)	(h)
A	1 x 10^{-1}	0.82	1.35	0.43	5.91	1.6	1.43	0.71	3.1
B	5 x 10^{-2}	0.40	3.1	0.91	11.97	3.18	2.96	1.20	5.0
C	1 x 10^{-2}	0.20	6.02	2.21	29.17	6.27	6.41	2.31	7.1
D	5 x 10^{-3}	0.16	8.45	2.65	30.60	9.11	8.14	3.52	10.8
E	1 x 10^{-3}	0.09	31.55	9.81	71.05	27.12	25.85	7.85	>24

2.2.3 Two-dimensional correlation analysis

To gain a more detailed insight into the performance of **FeL$_1$oct** in alkyd resin, the time-resolved infrared spectra were subjected to generalized two-dimensional (2D) correlation analysis. This approach enables simplification of complex spectra consisting of many overlapped peaks, enhancement of spectral resolution by spreading peaks over the second dimension and the determination of sequential order for processes related to fluctuations of given infrared bands.[23, 24] The theoretical background of 2D correlation analysis, including the summarization of possible applications, are reviewed elsewhere.[25] Briefly, the cross-correlated dynamic fluctuations of infrared signals at given wavenumbers (ν_1, ν_2) produce synchronous (Φ) and asynchronous (Ψ) 2D IR spectra. The sequential order of the changes at given wavenumbers (ν_1, ν_2) can be determined from signs of the cross-peaks using following Noda's rules:

a) If $\Phi(\nu_1, \nu_2) > 0$, $\Psi(\nu_1, \nu_2) > 0$ or if $\Phi(\nu_1, \nu_2) < 0$, $\Psi(\nu_1, \nu_2) < 0$,
then the movement of ν1 is before that of ν_2 ($\nu_1 \rightarrow \nu_2$).
b) If $\Phi(\nu_1, \nu_2) > 0$, $\Psi(\nu_1, \nu_2) < 0$ or if $\Phi(\nu_1, \nu_2) < 0$, $\Psi(\nu_1, \nu_2) > 0$,
then the movement of ν1 is after that of ν_2 ($\nu_1 \leftarrow \nu_2$).
c)If $\Phi(\nu_1, \nu_2) > 0$, $\Psi(\nu_1, \nu_2) = 0$ or if $\Phi(\nu_1, \nu_2) < 0$, $\Psi(\nu_1, \nu_2) = 0$,
then the movements of ν_1 and ν_2 are simultaneous ($\nu_1 \approx \nu_2$).
d) If $\Phi(\nu_1, \nu_2) = 0$, then sequential order cannot be determined.

The 2D correlation analysis of the time-resolved infrared spektra was focused mainly on a region of O-H stretching bands (3650–3100 cm^{-1}). The bands originate from carboxylic functions and secondary hydroxyl groups of the alkyd backbone

resulting from incomplete esterification upon the binder production. Nevertheless, our main attention was given to the hydroxyl-containing species appearing in the autoxidation process such as hydroperoxides, water and hydroxyl functions (Scheme 5).

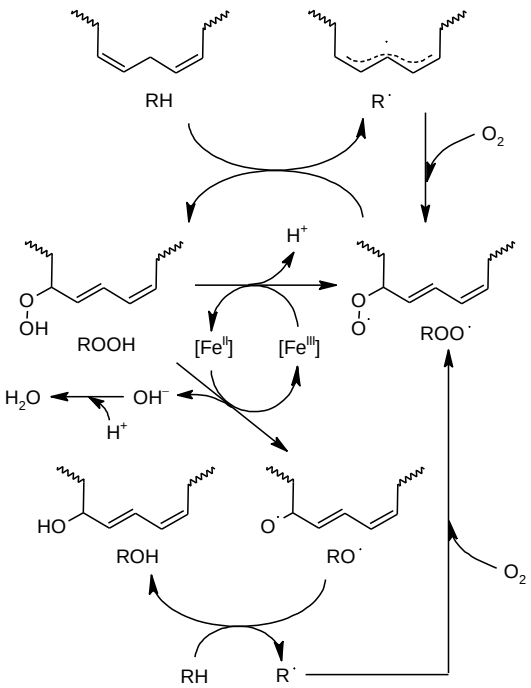

Scheme 4 Scheme of autoxidation process with using iron drier

Formulation **FeL$_1$oct/S50** at concentration 5 × 10−4 wt.% (run **E**) was found to be very suitable for 2D analysis since the autoxidation process is slow enough for catching the most important stages. The cross-peaks appearing in the asynchronous correlation spectra, shown in Figure 4, reveal the presence of three rising bands at 3520, 3410 and 3300 cm^{-1} those could be hardly resolved by common tools because they are overlapped and broadened.

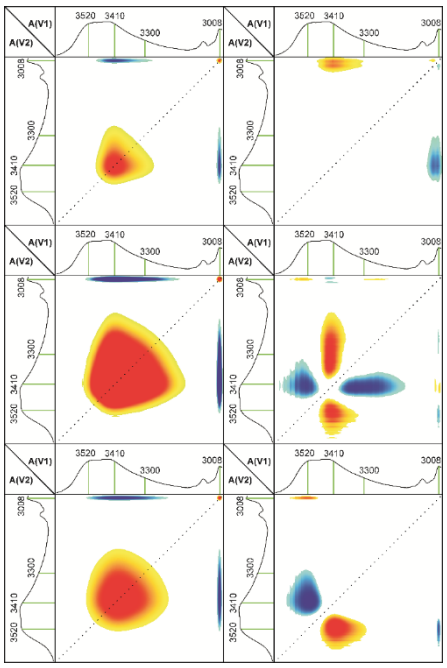

Figure 4 Synchronous (left) and asynchronous (right) correlations of the IR spectra in the region 3600–2995 cm^{-1}. Data of formulation: Fe-bispi/ S50 at metal concentration 5 ×10−4 wt.% collected at following periods: 0–50 min (first row), 50–150 min (second row) and 150–300 min (third row). Red and blue areas represent positive and negative correlation intensity, respectively.

In order to establish the detailed sequence order of consecutive reactions in the autoxidation process, the analyzed time scale has been divided into three periods. The 2D analysis of the spectra collected within the first 50 min reveals growth of the band at 3410 cm^{-1} that was assigned to O-H stretching of hydroperoxide function.[20] This band strongly correlates with CH stretching of the *cis*-CH=CH moiety (3008 cm^{-1}). As the corresponding synchronous and asynchronous cross-peaks are opposite in sign, the application of Noda's rules imply that the rise of band at 3410 cm^{-1} proceeds after the decrease of the band at 3008 cm^{-1} (3410←3008). Such observation indicates that the autoxidation process is initiated by the catalytic decomposition of hydroperoxides already present in the alkyd binder; see Scheme 5. The initiation of radical chain reaction producing ROOH from RH is related to consumption of ROOH at early stage of autoxidation process evident from slower development of the band at 3410 cm^{-1}. The analysis of the second period (t = 50–150 min) shows the appearance of water and alcohols those are the main byproducts of hydroperoxide decomposition.

The OH stretching modes of these species give two broad absorption bands at 3520 and 3300 cm^{-1} assignable to free and hydrogen- bonded hydroxyl groups, respectively. According to cross-peaks observed in the correlation spectra, both bands rise simultaneously after the band ascribed to ROOH:

$\Phi(3520, 3300) > 0$, $\Psi(3520, 3300) = 0$ imply (3520 ≈3300);
$\Phi(3410, 3520) > 0$, $\Psi(3410, 3520) > 0$ imply (3410 → 3520);
$\Phi(3410, 3300) > 0$, $\Psi(3410, 3300) > 0$ imply (3410 → 3300).

In the last period, suitable for the 2D correlation analysis (150–300 min), the growth of the band at 3300 cm^{-1} is almost ceased suggesting the saturation of available function groups in the alkyd backbone suitable for the effective hydrogen bonding. Similarly as in the second period, the development of band ascribed to hydroperoxides precedes the band at 3520 cm^{-1} (3410 → 3520). In summary, the sequence order of the bands at 3008, 3410, 3300 and 3520 cm^{-1} can be ambiguously assigned to following consecutive conversion: RH →ROOH →H2O + ROH. Such observation is fully in line with suggested catalytic function of **FeL_1oct** in alkyd binder, depicted in Scheme 5.

Detailed inspection of the 2D correlation spectra revealed noticeable changes in absorption bands at 2926, 2854, 1752, 1708, 1690 and 712 cm^{-1}. In accordance with previous studies, the band at 712 cm^{-1} was assigned to the in-plane bending mode of the *cis*-C=C-H moiety that is overlapped with the band of skeletal vibration mode of the $-(CH_2)_n-$ chain in the fatty acid tails.[21] This assignment was verified by 2D correlation analysis since the intensity of the band decreases synchronously with the consumption of active cis-double bonds in the course of autoxidation process [Φ(712, 3008) > 0, Ψ(712, 3008) = 0]. The bands at 2926 and 2854 cm^{-1} were assigned to the CH stretching of methylene groups in the fatty acid tails; see Table 3. The small decrease in intensity followed with shift toward higher wavelengths, apparent from typical pattern in the asynchronous spektra (Figure 5),[26] could be ascribed to modification in close neighborhood of CH_2 groups during autoxidation resulting in the change of the extinction coefficient and the energy of the vibration mode.

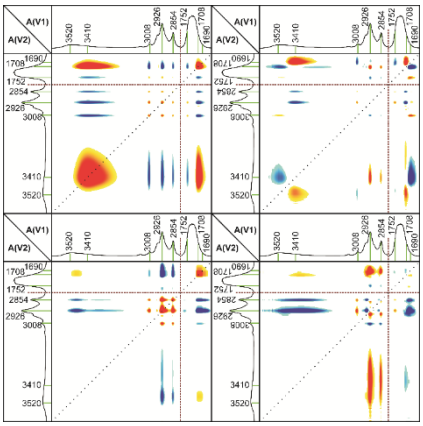

Figure 5 Synchronous (left) and asynchronous (right) correlations of the IR spectra in the regions 3650–2810 cm^{-1} and 1780–1650 cm^{-1}. Data of formulation: **FeL_1oct/S50** at metal concentration 5×10−3 wt.% collected at following periods: 0–100 min (first row) and 100–500 min (second row). Red and blue areas represent positive and negative correlation intensity, respectively

The analysis of the spectra in region of C=O stretching is rather difficult due to presence of broad and very intense bands originating from ester and carboxylic groups of the polyester backbone. The small decrease of the shoulder at 1752 cm^{-1} is not fully clarified but the rise of absorbance at 1708 and 1690 cm^{-1} is attributable to the

production of saturated and unsaturated aldehydes, respectively. These byproducts are formed mainly by β-scission of alkoxyl radicals, see Scheme 6.[27]

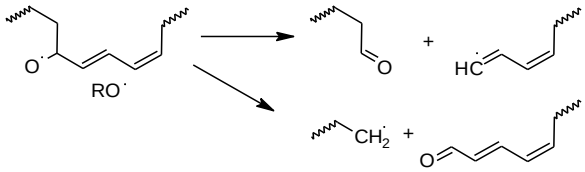

Scheme 5 Scheme of β-scission alkoxy radicals

The 2D correlation analysis verified that the band of unsaturated aldehyde well correlates with the band at 3520 cm^{-1} related to decay of ROOH. The application of Noda's rules further reveals different kinetic in development of the band assigned to saturated aldehydes that could be attributed to facile oxidation of these species during autoxidation proces.[28]

Conclusion

Currently, transition metal driers are used to accelerate the drying of alkyd resins. The most common driers are organic cobalt salts (e.g. cobalt 2-ethylhexanolate), which are now classified as reprotoxic (CMR2). These compounds could be reclassified as a class 1B carcinogen, which could lead to the prohibition of their using. Therefore, in some cases, cobalt driers can be replaced, for example by commercially available iron and manganese based driers.

Due to this fact, we decided to prepare the driers on based iron bispidine complexes, when we were inspirated by commercial bispidine iron complex manufactured by Borchers (**BORCHI®OXY – Coat**). We synthetized three substituted bispidine ligands (**L_1**, **L_2**, **L_3**), which served as intermediates for preparation of iron-based driers **FeL_1oct** and **FeL_2oct**. Unfortunately, we failed to prepare iron complex with ligand **L_3**.

The prepared complexes **FeL_1oct** and **FeL_2oct** are very soluble in non-polar solvent. Due to their yellow color, they can be used in light-pigmented paints. Further advantage is that they do not contain corrosion ionts. X-ray diffraction analysis described coordination sphere of iron in **FeL_1oct** and **FeL_2oct** as deformed octahedral.

Monitoring of drying activity of **FeL_1oct** and **FeL_2oct** was done on alkyd resins modified by soybean oil with different oil length (**S40**, **S50**, **S60**). At the same time we studied drying activity of prepared iron complexes **FeL_1oct** and **FeL_2oct** and drying influence of substituent on the pyridine ring.

If we compared performance of driers **FeL_1oct** and **FeL_2oct**, we find out higher drying activity of **FeL_1oct** in the system **S40** a **S50**, while both of driers reach very similar drying acitity in the system **S60**. As the optimal concentration for commercial using is considered the lowest concentration of drier, in which system exhibits tack-free time shorter than 8.5 h. At the same time we found that in tha case **FeL_1oct** and **FeL_2oct** is needed lower quantity than **Co-Nuodex**.

The obtained results showed that prepared complexes **FeL_1oct** and **FeL_2oct** can be used in wide range of concentrations. These complexes are not sensitive to

overdosing as observed for **Co-Nuodex**. The comparison of obtained data for **FeL_1oct** and **FeL_2oct** with commercial bispidine iron-based drier **BORCHI®OXY – Coat** reveals very similar activity in alkyd resins under the study. Only in case of **S60**, the commercial **BORCHI®OXY – Coat** does not give flat clar film but we observed a fine emulsion of alkyd resin and drier.

List of references

1. van Gorkum, R.; Bouwman, E., The oxidative drying of alkyd paint catalysed by metal complexes. *Coordination Chemistry Reviews* **2005,** *249*, 1709-1728.
2. Soucek, M.; Khattab, T.; Wu, J., Review of autoxidation and driers. *Progress in Organic Coatings* **2012,** *73*, 435-454.
3. Lison, D.; De Boeck, M.; Verougstraete, V.; Kirsch-Volders, M., Update on the genotoxicity and carcinogenicity of cobalt compounds. *Occup Environ Med* **2001,** *58*, 619-25.
4. De Boeck, M.; Kirsch-Volders, M.; Lison, D., Cobalt and antimony: genotoxicity and carcinogenicity. *Mutation Research/Fundamental and Molecular Mechanisms of Mutagenesis* **2003,** *533*, 135-152.
5. Warzeska, S. T.; Zonneveld, M.; van Gorkum, R.; Muizebelt, W. J.; Bouwman, E.; Reedijk, J., The influence of bipyridine on the drying of alkyd paints: a model study. *Progress in Organic Coatings* **2002,** *44*, 243-248.
6. Oyman, Z. O.; Ming, W.; Micciché, F.; Oostveen, E.; van Haveren, J.; van der Linde, R., A promising environmentally-friendly manganese-based catalyst for alkyd emulsion coatings. *Polymer* **2004,** *45*, 7431-7436.
7. Kalenda, P.; Holeček, J.; Veselý, D.; Erben, M., Influence of methyl groups on ferrocene on rate of drying of oxidizable paints by using model compounds. *Progress in Organic Coatings* **2006,** *56*, 111-113.
8. Šťava, V.; Erben, M.; Veselý, D.; Kalenda, P., Properties of metallocene complexes during the oxidative crosslinking of air drying coatings. *Journal of Physics and Chemistry of Solids* **2007,** *68*, 799-802.
9. Erben, M.; Veselý, D.; Vinklárek, J.; Honzíček, J., Acyl-substituted ferrocenes as driers for solvent-borne alkyd paints. *Journal of Molecular Catalysis A: Chemical* **2012,** *353–354*, 13-21.
10. de Boer, J. W.; Wesenhagen, P. V.; Wenker, E. C. M.; Maaijen, K.; Gol, F.; Gibbs, H.; Hage, R., The Quest for Cobalt-Free Alkyd Paint Driers. *European Journal of Inorganic Chemistry* **2013,** *2013*, 3581-3591.
11. Hage, R.; de Boer, J. W.; Gaulard, F.; Maaijen, K., Chapter Three - Manganese and Iron Bleaching and Oxidation Catalysts. In *Advances in Inorganic Chemistry*, van Eldik, R.; Hubbard, C. D., Eds. Academic Press2013; Vol. 65, pp 85-116.
12. Börzel, H.; Comba, P.; Hagen, K. S.; Lampeka, Y. D.; Lienke, A.; Linti, G.; Merz, M.; Pritzkow, H.; Tsymbal, L. V., Iron coordination chemistry with tetra-, penta- and hexadentate bispidine-type ligands. *Inorganica Chimica Acta* **2002,** *337*, 407-419.
13. Gezici-Koç, Ö.; Thomas, C. A. A. M.; Michel, M.-E. B.; Erich, S. J. F.; Huinink, H. P.; Flapper, J.; Duivenvoorde, F. L.; van der Ven, L. G. J.; Adan, O. C. G., In-depth study of drying solvent-borne alkyd coatings in presence of Mn- and Fe-based catalysts as cobalt alternatives. *Materials Today Communications* **2016,** *7*, 22-31.
14. Skalský, J., Preparation and application of drying agents in paints. *Progress in Organic Coatings* **1976,** *4*, 137-160.
15. Bieleman, J. H., Progress in the development of cobalt-free drier systems. *Macromolecular Symposia* **2002,** *187*, 811-822.

16. Miccichè, F.; van Haveren, J.; Oostveen, E.; Ming, W.; van der Linde, R., Oxidation and oligomerization of ethyl linoleate under the influence of the combination of ascorbic acid 6-palmitate/iron-2-ethylhexanoate. *Applied Catalysis A: General* **2006,** *297*, 174-181.
17. Holzgrabe, U.; Erciyas, E., Synthese und Stereochemie potentiell stark analgetischer 2,4-m-diarylsubstituierter 3,7-Diazabicyclo[3.3.1]nonan-9-on-1,5-diester. *Archiv der Pharmazie* **1992,** *325*, 657-663.
18. Comba, P.; Lopez de Laorden, C.; Pritzkow, H., Tuning the Properties of Copper(II) Complexes with Tetra- and Pentadentate Bispidine (=3,7-Diazabicyclo[3.3.1]nonane) Ligands. *Helvetica Chimica Acta* **2005,** *88*, 647-664.
19. Preininger, O.; Honzíček, J.; Kalenda, P.; Vinklárek, J., Drying activity of oxovanadium(IV) 2-ethylhexanoate in solvent-borne alkyd paints. *Journal of Coatings Technology and Research* **2016,** *13*, 479-487.
20. van de Voort, F. R.; Ismail, A. A.; Sedman, J.; Emo, G., Monitoring the oxidation of edible oils by Fourier transform infrared spectroscopy. *Journal of the American Oil Chemists' Society* **1994,** *71*, 243-253.
21. Okan Oyman, Z.; Ming, W.; van der Linde, R., Oxidation of model compound emulsions for alkyd paints under the influence of cobalt drier. *Progress in Organic Coatings* **2003,** *48*, 80-91.
22. Fjällström, P.; Andersson, B.; Nilsson, C.; Andersson, K., Drying of linseed oil paints: a laboratory study of aldehyde emissions. *Industrial Crops and Products* **2002,** *16*, 173-184.
23. Noda, I., Two-dimensional infrared spectroscopy. *Journal of the American Chemical Society* **1989,** *111*, 8116-8118.
24. Marcott, C.; Dowrey, A. E.; Noda, I., Dynamic two-dimensional IR spectroscopy. *Analytical Chemistry* **1994,** *66*, 1065A-1075A.
25. Noda, I., Two-Dimensional Infrared (2D IR) Spectroscopy: Theory and Applications. *Appl. Spectrosc.* **1990,** *44*, 550-561.
26. Morita, S.; Shinzawa, H.; Noda, I.; Ozaki, Y., Effect of band position shift on moving-window two-dimensional correlation spectroscopy. *Journal of Molecular Structure* **2006,** *799*, 16-22.
27. Nawar, W. W., Chemical changes in lipids produced by thermal processing. *Journal of Chemical Education* **1984,** *61*, 299.
28. Lazzari, M.; Chiantore, O., Drying and oxidative degradation of linseed oil. *Polymer Degradation and Stability* **1999,** *65*, 303-313.

List of Published Works

1) AUTOXIDATION OF ALKYD RESINS CATALYZED BY IRON(II) BISPIDINE COMPLEX: DRYING PERFORMANCE AND IN-DEPTH INFRARED STUDY, Martin Křižan, Jaromír Vinklárek, Milan Erben, Ivana Císařová, Jan Honzíček, *Progress in Organic Coatings*, **2017**, *111*, 361–370.

2) IRON(II) COMPLEX WITH MODIFIED BISPIDINE LIGAND: SYNTHESIS AND CATALYTIC ALKYD DRYING, Martin Křižan, Jaromír Vinklárek, Milan Erben, Zdeňka Růžičkova, Jan Honziček, *Inorganica Chimica Acta*, **2019**, *486*, 636–641.

List of Conference Contributions
Poster presentation

Křižan M., Erben M., Vinklárek J., THE STUDY OF DRYING ACTIVITY OF TRANSITION METAL BISPIDON COMPLEXES, ISAC13 Challenges in inorganic and material chemistry, Dublin – Ireland, June 1st – 4th, **2014**

Křižan M., Erben M., Kalenda P., Vinklárek J., INFRARED SPECTROSCOPY STUDY OF ALKYD AUTOXIDATION PROCES, APME 2015 IUPAC, Yokohama – Japan, October 18th – 22th, **2015**